



Numerical Analysis of Laminar and Permanent
Thermal Natural Convection in a Closed
Enclosure with Different Geometries and
Conditions

Si Abdalh Mayouf and Bouafia Sihem

EasyChair preprints are intended for rapid
dissemination of research results and are
integrated with the rest of EasyChair.

July 1, 2024



Proceedings of Extended Abstract TEMPLATE

Numerical analysis of laminar and permanent thermal natural convection in a closed enclosure with different conditions.

M. SiAdallah^{1*}, B. Sihem²

¹Physics Department, Faculty of Science, University of M'Sila, Algeria.

²Physics Department, Faculty of Science, University of M'Sila, Algeria.

1. ABSTRACT

In this study, we present a numerical analysis of laminar and permanent thermal natural convection in a closed enclosure with different conditions using FORTRAN language. The resulting system of algebraic equations was then solved using the iterative method with the Gauss-Seidel algorithm and relaxation. The results are presented in the form of isotherms, velocity and stream lines as a function of the Rayleigh number, as well as the Nusselt number. The findings indicate that an increase in the Rayleigh number leads to a higher convective heat transfer within the enclosure.

1. Introduction

The study of natural convection in closed enclosures has been the subject of many theoretical and experimental studies. Many published works have been developed concerning natural convection in different shapes of enclosures (either experimental or numerical) with different calculation methods and with different data and boundary conditions.

Sezai et al. [1] studied three-dimensional double diffusion natural convection in a cubic enclosure for thermal and solute gradients at opposite horizontals. They indicate that doubly diffusive flow in cavities with opposite volume forces is strictly three-dimensional for a certain range of parameters.

Akrour et al. [2] made a numerical study of natural thermo solutal convection in a rectangular enclosure, the horizontal walls of the enclosure are heated and cooled and a vertical concentration gradient is imposed. The objective of their investigation is to identify the thermal or solutal-dominated flow regime. They found that it is possible to obtain several solutions which essentially depend on the initial conditions. Also, the results reveal that for a stratified fluid, a conductive heat transfer occurs at the expense of thermal convection.

Aydin and Yang [3] numerically studied natural laminar air convection in a two-dimensional, rectangular enclosure with localized heating below and symmetrical cooling on the sides. Their analysis included the influence of the length of the heated part and Ra on heat transfer. They found that the flow and temperature fields are symmetric because of the symmetry of the boundary conditions.

*Corresponding Author: mayouf.siabdallah@univ-msila.dz

Kuznetsov et al. [4] examined the natural double diffusive convection inside a cubic cavity where lower wall is isothermal and maintained at a uniform concentration and the other walls are adiabatic and impermeable. They examined the influence of the Rayleigh number on the flow and rate of heat and mass transfer, the influence of the conductivity ratio on the heat and mass transfer and the effect of the sources size of heat and mass on mass transfer regimes.

Nikbakhti et al. [5] numerically analyzed the heat and mass transfer for air contained in a rectangular enclosure with partially thermally active walls. Teamah et al. [6] numerically studied a double diffusion flow of natural convection in an inclined rectangular enclosure in the presence of a magnetic field and a heat source. The authors concluded that: the inclination angle affects the buoyancy forces and the magnetic field reduces heat transfer and fluid circulation due to the delay effect of the electromagnetic body force.

2. Mathematical model

The physical problem considered is schematized in figure 1. It is a closed two-dimensional enclosure of height H . The flow in the enclosure is due to the temperature difference and therefore to the density difference which leads to convective flow.

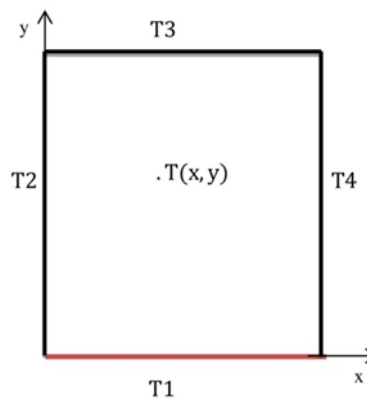


Fig. 1 Fig. 1 Model of closed enclosure with boundary conditions

2.1 General hypotheses

The following hypotheses used are:

- Fluid flow and heat transfer are permanent and the regime is laminar.
- The flow is assumed to be two-dimensional (2D).
- The fluid is Newtonian and incompressible
- The physical properties of the fluids are assumed to be constant.
- Heat transfer by radiation is negligible.

2.2 Governing equations

2.2.1 Dimensionless vorticity equation

To eliminate the pressure terms in the motion equation, we use the dimensionless vorticity equation W defined by:

$$U \frac{\partial W}{\partial X} + V \frac{\partial W}{\partial Y} = \frac{Ra}{Pr} \frac{\partial \theta}{\partial X} + \left(\frac{\partial^2 W}{\partial X^2} + \frac{\partial^2 W}{\partial Y^2} \right) \quad (1)$$

The vorticity equation the following dimensionless variables:

$$X = \frac{x}{L}, \quad Y = \frac{y}{L}, \quad U = \frac{u}{(\frac{v}{L})}, \quad V = \frac{v}{(\frac{v}{L})}, \quad \theta = \frac{T-T_0}{T_p-T_0}, \quad P = \frac{p}{\rho_0(\frac{v}{L})^2} \quad (2)$$

Using Eq.2, the dimensionless continuity and energy equations can be written as:

2.2.2 Dimensionless continuity equation

$$\frac{\partial U}{\partial X} + \frac{\partial V}{\partial Y} = 0 \quad (3)$$

2.2.3 Dimensionless energy equation

$$U \frac{\partial \theta}{\partial X} + V \frac{\partial \theta}{\partial Y} = \frac{1}{Pr} \left(\frac{\partial^2 \theta}{\partial X^2} + \frac{\partial^2 \theta}{\partial Y^2} \right) \quad (4)$$

2.2.4 Stream function

The dimensionless stream function is defined by:

$$U = \frac{\partial \psi}{\partial Y}, \quad V = -\frac{\partial \psi}{\partial X} \quad (5)$$

2.2.5 Boundary conditions

By using the fig.2, the boundary conditions used are:

$$\begin{aligned} 0 \leq X \leq 1, Y=0, U=V=0, \quad \theta = \theta_1 = 1 \\ X=0, 0 \leq Y \leq 1, U=V=0, \quad \theta = \theta_2 = 0 \\ 0 \leq X \leq 1, Y=1, U=V=0, \quad \theta = \theta_3 = 0 \\ X=1, 0 \leq Y \leq 1, U=V=0, \quad \theta = \theta_4 = 0 \end{aligned}$$

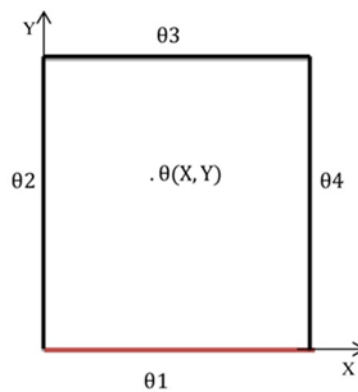


Fig. 2 Model of closed enclosure with dimensionless boundary conditions

2.2.6 Nusselt number

The Nusselt number is used to characterize heat transfers between a fluid and a wall, called convective transfer. It is defined as follows:

$$Nu = -\left(\frac{\partial\theta}{\partial Y}\right)_{Y=0} \tag{6}$$

3. Numerical formulation

To resolve numerically the above equations, various numerical methods are used. Among these methods, we can cite the method of finite differences, finite elements and finite volumes, in addition to a variety of software present on the market. To carry out our numerical simulations, we opted for a calculation program written in FORTRAN language based on the finite difference method.

3.1 Mesh

The method of discretizing of the partial differential equations requires the choice of a geometry mesh (Fig.3). If we take any function ϕ and using Taylor series development and with the finite difference method in the vicinity of the point P(i, j) in the scheme presented in Fig. (4),

We use this technique to transform the system of partial differential equations into a system of algebraic equations (discretization) which will be solved by the appropriate methods.

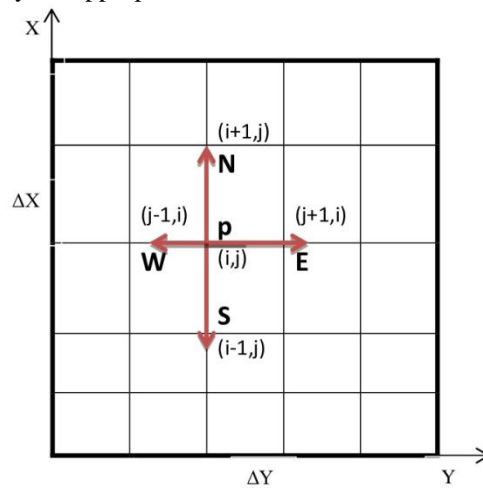


Fig.4 Mech scheme

3.1 Discretization of the general equation

By using a general function Φ which can designate W and θ , equations (1) and (4) can be grouped into a single equation obeying the following expression:

$$U\frac{\partial\Phi}{\partial X} + V\frac{\partial\Phi}{\partial Y} - A\left(\frac{\partial^2\Phi}{\partial X^2} + \frac{\partial^2\Phi}{\partial Y^2}\right) = S \tag{7}$$

For $\Phi = W$, $A=1$, $S = S = -\frac{Ra}{Pr} \frac{\partial\theta}{\partial Y}$

For $\Phi = \theta$, $A=1$, $\frac{1}{Pr}$, $S=0$

Using the finite difference, equations 7 can be discretized as follow:

$$U_j^i \frac{\Phi_j^{i+1} - \Phi_j^{i-1}}{2\Delta X} + V_j^i \frac{\Phi_{j+1}^i - \Phi_{j-1}^i}{2\Delta Y} - A\left(\frac{\Phi_j^{i+1} - 2\Phi_j^i + \Phi_j^{i-1}}{\Delta X^2} + \frac{\Phi_{j+1}^i - 2\Phi_j^i + \Phi_{j-1}^i}{\Delta Y^2}\right) = S \tag{8}$$

3.2 Method of resolution

To solve the previous equations, we use iterative methods and we choose the Gauss-Seidel method with relaxation.

Applied this method on Eq. 8, we obtain,

$$(\Phi_P)^{K+1} = \frac{A_E(\Phi_E)^K + A_W(\Phi_W)^K + A_S(\Phi_S)^K + A_N(\Phi_N)^K + S}{A_P} \quad (9)$$

The coefficients A_N, A_E, A_W, A_S , and A_P are different from one equation to another. Their values are defined from equation (8) as follows:

$$A_P = 2A \left(\frac{1}{\Delta X^2} + \frac{1}{\Delta Y^2} \right) \quad (10)$$

$$A_S = -\frac{U_j^i}{2\Delta X} + \frac{A}{\Delta X^2} \quad (11)$$

$$A_N = \frac{A}{\Delta X^2} - \frac{U_j^i}{2\Delta X} \quad (12)$$

$$A_E = \frac{A}{\Delta Y^2} + \frac{V_j^i}{2\Delta Y} \quad (13)$$

$$A_W = \frac{V_j^i}{2\Delta Y} + \frac{A}{\Delta Y^2} \quad (14)$$

Calculation of these parameters leads to calculate the stream function, the vorticity, and the velocity components U and V . The calculation converged if the following test is verified:

$$\left| \frac{\sum_{i=1}^{I_{max}} \sum_{j=1}^{J_{max}} (\Phi_p)^{K+1} - \sum_{i=1}^{I_{max}} \sum_{j=1}^{J_{max}} (\Phi_p)^K}{\sum_{i=1}^{I_{max}} \sum_{j=1}^{J_{max}} (\Phi_p)^K} \right| \leq 10^{-4} \quad (15)$$

4. Results and discussion

4.1 Choice of the mesh of the discretization grid

A preliminary calculation of the temperature field for ($Y=1/2$) using three different meshes gave almost identical results (Fig.4).

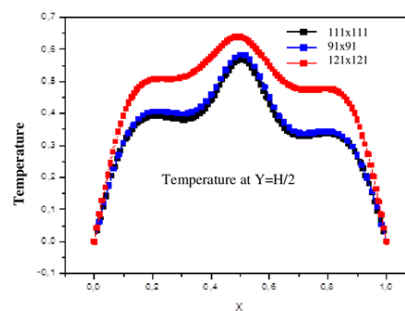


Fig.4 temperature field for different meshes

4.3 Stream lines

Figure (5) shows the structure of the streamlines for different values of the Rayleigh number. We notice a formation of two counter-rotating cells, one rotates clockwise and the second rotates counterclockwise as shown in figure (5.e) for all cases. We also notice that the configuration presents a symmetrical flow characterized by two identical counter-rotating cells because the boundary conditions are symmetrical. This physical phenomenon can be translated as follows: The fluid which is heated by the lower wall moves towards the cold upper wall, where it divides into two flows, one goes towards the left vertical cold wall and the other moves towards the right vertical cold wall, the two cells are almost equal. It should be noted that for a given Rayleigh number, the streamlines are almost identical when varied. The intensity of the flow therefore remains the same value for a fixed Rayleigh number. We notice that with the increase in the Rayleigh number, the intensity of the recirculation inside the enclosure increases and the centers of the current lines move upwards.

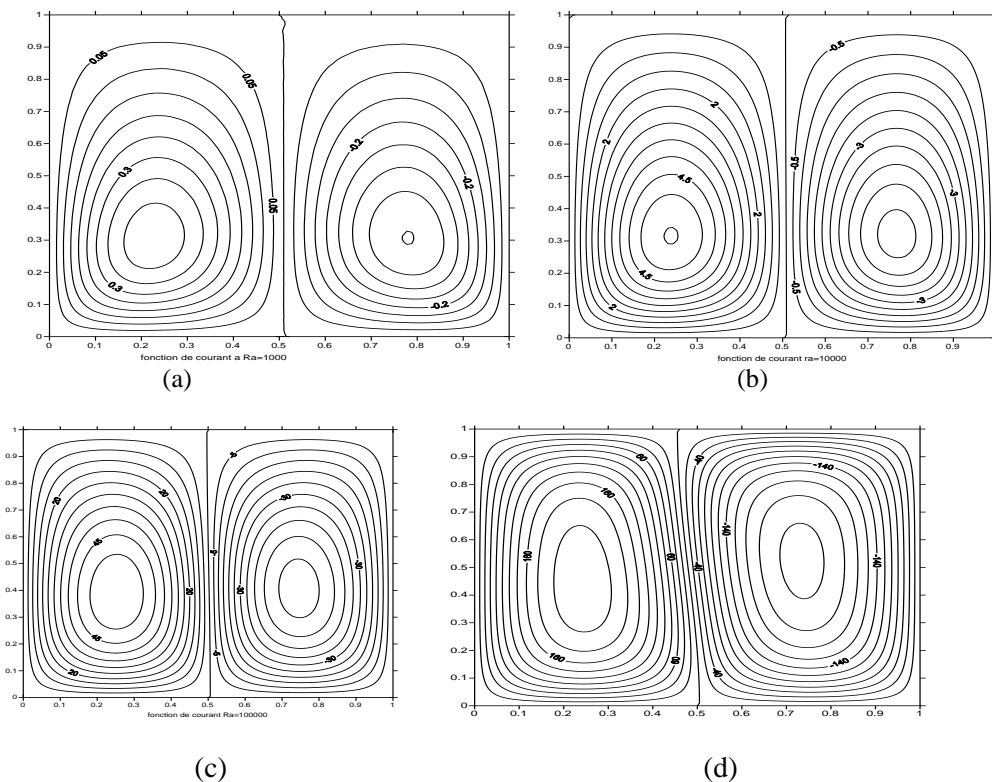


Figure 5. Streamlines for different values of the Rayleigh number

(a) $Ra=10^3$, (b) $Ra=10^4$, (c) $Ra=10^5$, (d) $Ra=10^6$

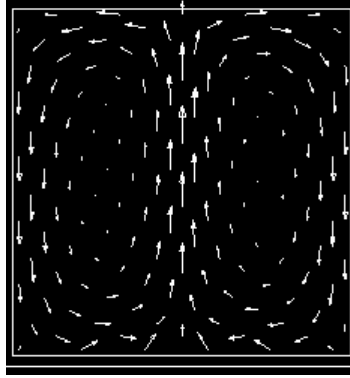


Figure 5.e flow structure

4.4 Temperature profile (isotherms)

Figure (6) reflects the phenomenon of natural convection. The isotherms show that the heat recovered from the hot base of the enclosure is transformed by natural convection upwards to the middle of the enclosure by the pair of cells in the center. This explains the relatively high temperatures in the central part of the enclosure. Heat is dissipated equally through both side walls due to symmetry. For $Ra = 10^3$, the isotherms become almost concentric ellipses and have a symmetrical structure with respect to the passing vertical plane thus these isotherms show that heat transfer by conduction is predominant (absence of transfer by convection). When $Ra = 10^4$, the deformation of the isotherms increases. When $Ra = 10^6$, the thermal boundary layers become thinner and the isotherms become stratified. The increase in the Rayleigh number causes the isotherms to move closer to each other in the zone located near the heated lower wall, i.e. the temperature gradients become higher near the heated lower wall. This implies an increase in heat transfer through the bottom wall of the enclosure for a higher Rayleigh number. Therefore, the highest temperatures are those of the fluid flowing parallel to the heated wall, while the lowest temperatures are those of the fluid flowing parallel to the cold walls [43].

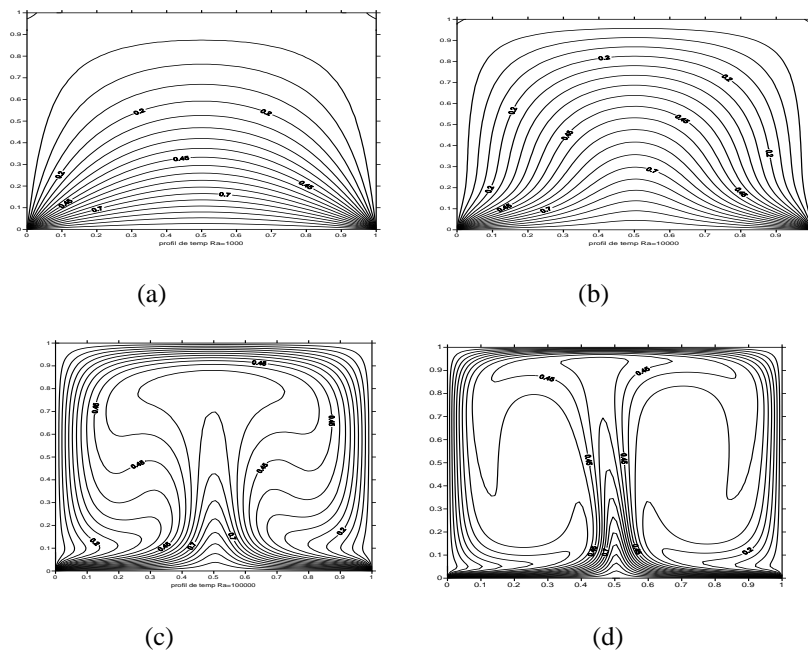


Figure 6: Structure of isotherms for different values named Rayleigh.

(a) $Ra= 10^3$, (b) $Ra= 10^4$, (c) $Ra= 10^5$, (d) $Ra= 10^6$

4.5 Velocity profile

Figure (7) illustrates the vertical velocity structure of fluid flow for different Rayleigh numbers. We notice a descent of the fluid at the level of the cold side walls and an increase at the level of the heated wall as also shown in figure (7.e). This elevation increases with the increase in the Rayleigh number and reaches its maximum at the center of the heated wall, where the temperature is higher. This is due to the increase in the intensity of thermal thrust forces and therefore to the predominance of heat transfer by convection.

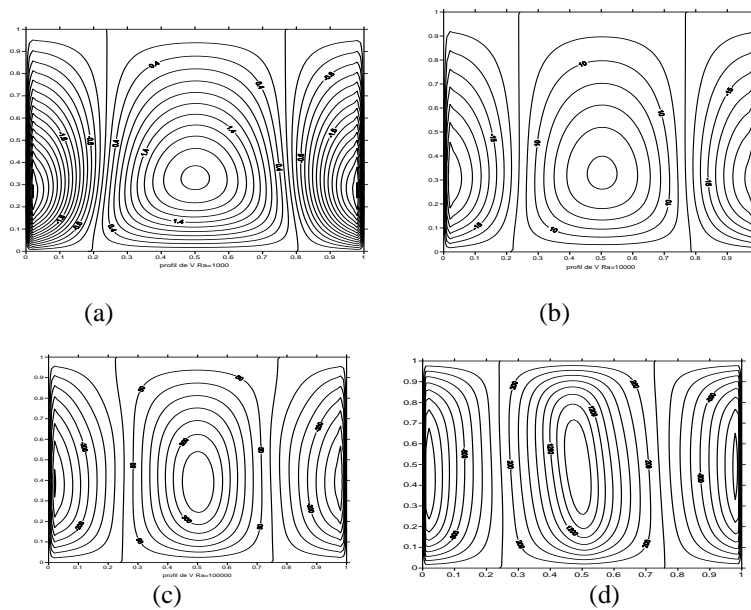


Figure 7: Structure of vertical velocity for different values of the Rayleigh number.

(a) $Ra= 103$, (b) $Ra= 104$, (c) $Ra= 105$, (d) $Ra= 106$

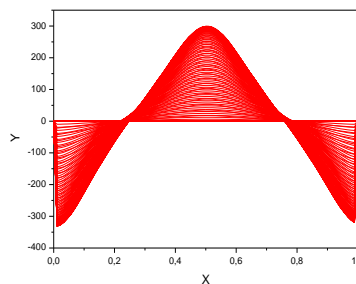


Figure 7.e : vertical speed profiles for $Ra=10^5$

4.6. Local Nusselt number

Figure (8) illustrates the variation of the local Nusselt number on the active (hot) wall whatever the value of the Rayleigh number. We notice in this figure, zero values of the Nusselt number in the middle of the hot part that this is

where the temperature gradient is the lowest and the heat transfer between the hot wall and the fluid takes place only by conduction, on the other hand, its maximum value at the terminals of the heated source given that this corresponds to the contact of the cold fluid coming from the side walls with the ends of the heated source, which will give rise to the strongest temperature gradients.

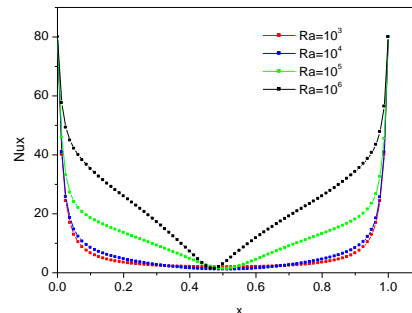


Figure 8: variation of the Nusselt number as a function of X

Conclusion

In this work, we presented a numerical study of heat transfer by natural convection in closed enclosure filled by air. The lower base of this cavity is kept hot (as a heat source) at a constant temperature and the other walls are cold at a constant temperature.

Numerical simulation using FORTRAN are carried out for different Rayleigh numbers. The resolution of the equations governing flow and heat transfer was approached by the finite difference method with the relaxation method.

The results obtained show that:

- Increasing the Rayleigh number favors heat transfer in the cavity given the increase in convection currents and therefore the speed.
- For a low Rayleigh number, of the order of 10^3 , we notice dominance of the mode of heat transfer by conduction. Beyond this value, convection dominates and appears more clearly for $Ra=10^5$.
- The flow regime always remains laminar for the range of the Rayleigh number considered.
- The Nusselt number increases with increasing Rayleigh number.

References

- [1] Sezai and A.A. Mohamad, *Double diffusive convection in a cubic enclosure with opposing temperature and concentration gradient*, "Phys. Fluids, vol. 12, pp. 2210-2223, 2000.
- [2] D. Akrou, *"Effet d'hystérésis en convection thermosolutale avec des gradients croisés: Etang de stockage"*, "Rev. Energ. Ren, vol. 3, pp. 39- 47, 2000.
- [3] O. Aydin and W. Yang. *"Natural convection in enclosures with localized heating from below and symmetrical cooling from sides"*. Int. J. Numerical methods for heat & Fluid flow, vol. 10 No.5, pp. 518-529.(2000).
- [4] G.V. Kuznetsov and M.A. Sheremet, *A numerical simulation of double-diffusive conjugate natural convection in an enclosure*, "Int. J. Thermal.Sci, vol. 50, pp. 1878-1886, 2011.
- [5] R. Nikbakhti and A. B. Rahimi, *Double-diffusive natural convection in a rectangular cavity with partially thermally active side walls*, "Journal of the Taiwan Institute of Chemical Engineers, vol. 43 (4), pp. 535-541, 2012.
- [6] A. Teamah, A.F. Elsafty and E.Z. Massoud, *Numerical simulation of double-diffusive natural convective flow in an inclined rectangular enclosure in the presence of magnetic field and heat source*, Int. J. Therm. Sci, vol. 52, pp. 161-175, 2012.